The dependence of light extraction improvement on optimized surface microstructure for AlGaN-based UVC-LEDs considering TM-polarized emission

Zhu, Yifan; Lu, Huimin; Wang, Jianping; Yu, Tongjun; Li, Zizheng; Tian, Yucheng

DOI
10.1016/j.micrna.2023.207614

Publication date
2023

Document Version
Final published version

Published in
Micro and Nanostructures

Micro and Nanostructures 181 (2023) 207614

Contents lists available at ScienceDirect

Micro and Nanostructures

journal homepage: www.journals.elsevier.com/micro-and-nanostructures

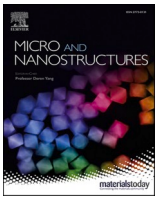

The dependence of light extraction improvement on optimized surface microstructure for AlGaN-based UVC-LEDs considering TM-polarized emission

Yifan Zhu [a], Huimin Lu [a,b], Jianping Wang [a,b,*], Tongjun Yu [c], Zizheng Li [d], Yucheng Tian [c]

[a] The School of Computer and Communication Engineering, University of Science and Technology Beijing, Beijing, 100089, China
[b] Shunde Innovation School, University of Science and Technology Beijing, Foshan, 528000, China
[c] The State Key Laboratory for Mesoscopic Physics, School of Physics, Peking University, Beijing, 100089, China
[d] Faculty of Applied Sciences, Delft University of Technology, 2628 CJ, Delft, the Netherlands

ARTICLE INFO

Keywords:
Ultraviolet light emitting diodes
Light extraction efficiency
Polarized component

ABSTRACT

In order to improve the light extraction of AlGaN-based short wavelength ultraviolet light emitting diodes (DUC-LEDs), a type of microstructure with high aspect ratio is introduced and optimized on the AlN substrate surface. And, particle swarm optimization (PSO) algorithm is used to inverse design of the surface microstructure to maximize the light extraction efficiency (LEE). Considering that the propagation characteristics of TM-polarized light are different from that of TE-polarized light, the optical field distribution and LEE is analyzed for the UVC-LEDs with different TE-polarized component when the optimized surface microstructure is applied. Furthermore, the preparation process tolerance of the high aspect ratio structure is discussed by calculating the LED's LEE when the structural deviation occurs or morphology changes. Simulation results show that, by using the optimized surface microstructure based on parabola cone array, the LEDs' LEE is increased from 4.4% to 8.7% and from 0.4% to 3.7% for TE-polarized and TM-polarized emission, respectively. In addition, it is demonstrated that the light extraction improvement by the surface microstructure has a good tolerance to the structural deviation and morphology. The results are significant for improving light extraction and realizing high efficient short wavelength AlGaN-based UVC-LEDs by designing surface microstructures.

1. Introduction

Ultraviolet (UV) light has a wide range of applications or potential applications in non-line-of-sight (NLOS) UV-communication, water purification, UV curing, medical treatment, plant lighting, optical sensing, lithography and other fields [1–6]. Especially the UVC (200–280 nm) part of the solar spectrum is strongly attenuated in the earth's atmosphere, which brings about an almost interference free space atmospheric channel and a no defense mechanism for organisms to high-energy photon exposure. Recently, it is reported that UVC light below 250 nm are human friendly compared with that above 250 nm [7–11]. Furthermore, the scattering of

* Corresponding author. The School of Computer and Communication Engineering, University of Science and Technology Beijing, Beijing, 100089, China.
E-mail address: jpwang@ustb.edu.cn (J. Wang).

https://doi.org/10.1016/j.micrna.2023.207614
Received 27 March 2023; Received in revised form 5 May 2023; Accepted 23 May 2023
Available online 24 May 2023

UVC light increases as the wavelength becomes shorter, leading to the performance improvement of NLOS UV communication system [12]. At present, AlGaN-based light emitting diodes (LEDs) has become the mainstream UVC light source due to its small size, energy saving, long life, stable performance and environment friendly. Several teams have fabricated AlGaN-based UVC-LEDs with peak emission wavelength about 220 nm, 233 nm, 247 nm, 250 nm, or even 210 nm [13–17]. However, the external quantum efficiency (EQE) decreases as the wavelength becomes shorter, and the EQE of UVC-LEDs with 210 nm emitting is only about 10^{-6} [17]. Thus, AlGaN-based UVC-LEDs suffer from low EQE and light output power (LOP), which becomes more serious as the wavelength becomes shorter, resulting in the application limit in great degree [18–20].

The low EQE of AlGaN-based UVC-LEDs is mainly contributed from the internal quantum efficiency (IQE) and light extraction efficiency (LEE). By improving epitaxial growth technology and designing active region structure, UVC-LEDs' IQE has been effectively enhanced to more than 80% [21,22]. Moreover, the low EQE is primarily due to the very low LEE for the AlGaN-based UVC-LEDs. It is revealed that as the Al component in AlGaN quantum wells (QWs) increases, the polarization of the transmitted light switches from the TE mode to the TM mode [23–27]. The TE-polarized emission can be improved by using compression strain, narrow quantum well layer, high aluminum mole fraction barrier or MQW structures [28–30]. However, for short wavelength UVC-LEDs, the TM-polarized component cannot be ignored, which will influence the light propagation and extraction [31]. Furthermore, a large number of UVC photons radiating to the p-region are absorbed by the p-type GaN and reflected by the substrate due to total reflection [32]. It is reported that LEE have improved by adding reflective p-electrodes [33], patterning the substrate [34], especially designing the surface structure [35,36]. However, the deviation in fabrication process is so easily produced for the designed surface microstructure to improve UVC-LEDs' LEE. Therefore, the LEE improvement based on surface structure design can be affected when both the TM-polarized light and fabrication error cannot be ignored for the AlGaN-based UVC-LEDs with a shorter emission wavelength.

In this work, a type of microstructure with high aspect ratio is designed on the AlN substrate surface to improve light extraction for 248 nm AlGaN-based UVC-LEDs with TE-polarized and TM-polarized emission. On this basis, the dependence of the light exaction on the optimized surface microstructure considering the optical polarization property is further investigated. The optical field distribution and LEE is analyzed for the UVC-LEDs with different TE-polarized component. The preparation process tolerance of the high aspect ratio structure is discussed by calculating the LED's LEE when the structural parameters have fluctuation. In addition, the influence of the microstructure morphology on the UVC-LED's LEE result is also explored.

2. Modeling and simulation

In group III nitride semiconductors, the conduction band is a fully symmetric *s*-orbital, while the valence band is formed by the *p*-orbital. The three valence subbands in the non strained system have *p*-orbital dipole distributions aligned along the *x*-axis, *y*-axis, and *z*-axis. The p_x and p_y orbits merge to form heavy hole (HH) and light hole (LH) hole entrainment (waveform $|X \pm Y|$ shape), with a symmetrical distribution rotating around the *c* [0001] axis. The transition from conduction to this HH and LH subband will generate TE-polarized light in the crystal. The p_z orbit forms a crystal-field split off (CH) subband (waveform $|Z|$ shape) along the *c*-axis direction, to which the transition will produce emission light with TM-polarized. Therefore, according to the thermal occupation of Fermi Dirac distribution, the optical polarization properties of the LEDs based on III nitride semiconductors are determined by the valence subband structure including energy-level order. Especially for Al-rich AlGaN-based quantum wells (QWs) used in UVC-LEDs, the CH subband is close to HH and LH subband, even became the first valence subband, leading to the increase of TM-polarized component in emission light. Among the influencing factors, quantum well structure, compressive strain, Al composition and other factors will have a greater impact on the TE-polarized component. Fig. 1 gives the original light field distribution for the emission light with different TE-polarized component, which is very different and sure to impact the light extraction from AlGaN-based UVC-LEDs.

In order to investigate the influence of the surface microstructure on light extraction for AlGaN-based UVC-LEDs considering optical polarization characteristic, a 3D-FDTD solutions software is used to calculate the propagation process including refraction, scattering, reflection and absorption. The selection of AlN material as the substrate for AlGaN-based UVC-LEDs can improve the crystal quality issues caused by lattice mismatch, which is currently the focus of researchers' efforts. Therefore, this article chooses the inverted structure model of AlN substrate [37,38]. Fig. 2(a) shows the schematic diagram of UVC-LEDs with surface microstructure

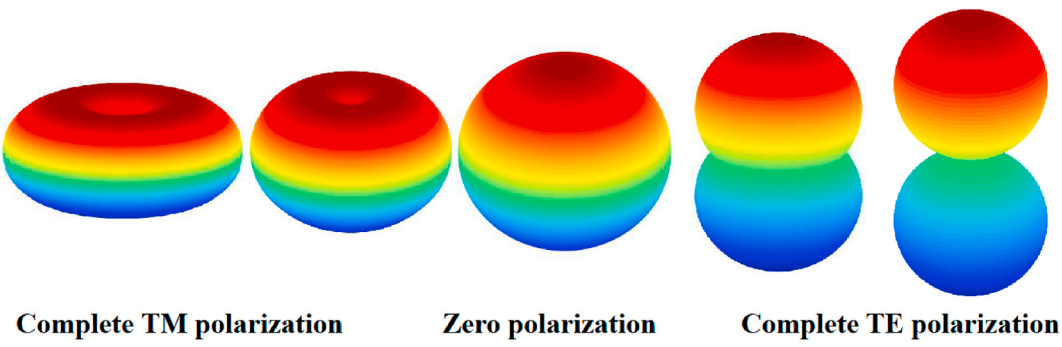

Fig. 1. Schematic diagram of original light field distribution for the emission light with different TE-polarized component.

based on parabola cone array in the simulation, without regard to the effect of electrode, current diffusion and other factors. Specifically, the UVC-LEDs model of flip chip includes a 2 μm thick AlN substrate, a 2 μm thick n-AlGaN layer, a 100 nm thick MQW layer, a 125 nm thick *p*-AlGaN layer as active region, and a 100 nm thick p-GaN layer. In this work, the parabola cone structure as a surface microstructure with high aspect ratio is used, which is expected to obtain more light incidence angles to a large extent. For the surface microstructure based on parabola cone array, let the diameter of the conical bottom be *d* and the array period be *T* as shown in Fig. 2 (b). And, the filling factor of the conical pattern is defined as the ratio of diameter to period (*d*/*T*) and the height of cone structure is *h*. In this study, epitaxial wafers of AlGaN-based UVC-LEDs can be grown on an AlN substrate, including $Al_{0.57}Ga_{0.43}N/Al_{0.74}Ga_{0.26}N$ for 248 nm emission [39]. When the compression stress or well width changes, the emission polarization ratio will change.

In simulation, limited by the calculation memory, the lateral dimension of the LEDs' model is set to 4 μm × 4 μm, which can be equivalent to large size model by setting the boundary conditions of the four transverse boundaries as metal boundary with 100% reflectivity [40]. And, the boundary conditions at the bottom and top are set as perfectly matched layers (PML) to fully absorb electromagnetic energy [41]. The relevant parameters of AlGaN are derived from the linear combination of AlN and GaN components in Ref. [42]. The absorption coefficients of n-AlGaN, MQW and GaN layers are 17 cm^{-1}, 1700 cm^{-1} and 300000 cm^{-1} respectively [43,44]. The refractive index of AlN substrate, AlGaN and GaN layers are set to 2.4, 2.6 and 2.7 respectively [45,46]. The array structure is on the surface of AlN substrate. The dipole is used as the light source and placed in the middle of the MQW region, with a peak emission wavelength of 248 nm and a half-width of 10 nm [47]. TE-polarized and TM-polarized emission are defined as electric dipoles oscillating perpendicular to the *c*-axis and oscillating parallel to the *c*-axis, respectively. A power monitor is placed at 50 nm above the surface microstructure to collect power transmission and record near-field radiation, which can be converted into far-field light distribution through Fourier transform. The Poynting vector integral of light distribution in each grid cell is the output power. Therefore, LEDs' LEE is defined as the ratio of the total extracted power collected from the power monitor to the total optical power emitted by the dipole source as shown below.

$$T(f) = \frac{\frac{1}{2}\int_{monitor} \mathrm{Re}(\mathrm{P}(f))\mathrm{dS}}{sourcepower(f)} \tag{1}$$

3. Results and discussions

As mentioned above, the TM-polarized component increases as the peak wavelength becomes shorter in the emission light of AlGaN-based UVC-LEDs. In order to investigate the influence of optical polarization on the light extraction from the LEDs with 248 nm peak wavelength, the surface microstructure is designed for the TE and TM-polarized emission light, respectively. With the help of intelligent algorithm, the device inverse design can be completed. It makes data processing, automatic execution simulation, parameter optimization, drawing and high-performance calculation processes have higher degrees of freedom. In this work, a reverse design method based on intelligent algorithm and 3D-FDTD simulation is used in the surface microstructure optimization to maximize the UVC-LEDs' LEE. And, considering the huge amount of computation caused by the complexity of mesh generation of UV wave and surface microstructure in 3D-FDTD, the particle swarm optimization (PSO) algorithm with fast convergence speed is selected in this work, which can find a group of parameter values as the optimal solution through multiple iterations and avoid convergence to the local optimal [48–51]. In the iterative process of optimized design for a surface microstructure based on parabola cone array, new particles with parameters *h*, *d* and *T* value are randomly generated repeatedly, and finally the optimal parameters for the maximized LEE value is obtained. To reduce the complexity of 3D-FDTD simulation and array structure parameters, the particle number *N* is set to 6. The optimization method has been described in Ref. [52], and the flow chart of the combination of PSO algorithm and FDTD is given. It is demonstrated that although the PSO algorithm is a random search process and each optimization process is inconsistent, the variance of the optimization results is less than 2% and the optimization usually stops about 10 iterations in the surface microstructure design for the AlGaN-based UVC-LEDs.

In order to maximize the light extraction of the UVC-LEDs with 248 nm peak emission wavelength, the optimization process of

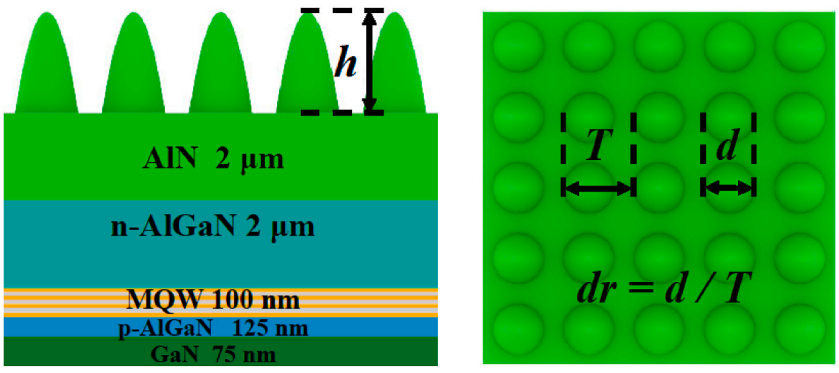

Fig. 2. Schematic diagram of the AlGaN-based UVC-LEDs with surface microstructure based on parabola cone array. The diameter of the conical bottom is *d*, the array period is *T*, and the height of the conical structure is *h*.

surface microstructure based on parabola cone array is given in Fig. 3 for the TE-polarized and TM-polarized light, respectively. It is can be seen that by using the optimized surface microstructure, the LEDs' LEE for TE-polarized emission is increased from 4.4% to 8.7% as shown by the red solid line with empty circle symbol in Fig. 3. Furthermore, as given in the blue curve and triangle symbol, the LEE of UVC-LEDs with TM-polarized emission is improved from 0.4% to 3.7% with a significant increase of 820% after optimizing surface microstructure. After iteration, the final optimization result of TE-polarized emission shows that the conical bottom d is 230 nm, the array period T is 230 nm, and the structural height h is 3 μm.And the optimization result of TM-polarized emission shows that the bottom of the conical bottom d is 498 nm, the array period T is 560 nm, and the structural height h is 3 μm. The illustration in Fig. 3 also shows the adjustment process of each structural parameter value in the optimization, where the scattered points represent the particles used by each generation of optimal value. In order to intuitively understand the structural parameter optimization process of the optimal value, a broken line is used to connect the parameter values selected by the optimal result of each generation. It can be seen from the figure that after 5–6 iterations, LEE obtained the optimal value. Subsequently, 2–3 generations of particles will continue to search to avoid falling into local optima. Finally, the particles gradually converge near the optimal structural parameters. It is concluded that the optimization trend of each parameter value changes with the iteration but tends to be stable at an optimal value after several iterations, from which an obvious advantage on suppressing local optimization is reflected due to the introduction of the PSO algorithm. As a result, by using the optimized surface microstructure, the LEE can be significantly enhanced for the AlGaN-based UVC-LEDs with TE-polarized or TM-polarized emission.

For the AlGaN-based UVC-LEDs with different proportion of TE-polarized emission, the LEE is further investigated when different optimized surface microstructure is applied. As shown in Fig. 4, the red curve with triangle symbol and blue curve with circle symbol give the LEDs' LEE varying with the percent of TE-polarized component by using the surface microstructure optimized for TE-polarized and TM-polarized emission, respectively. On this basis, the surface microstructure for the optimal LEDs' LEE for different TE-polarized component can be obtained as shown in the green line with rhombus symbol in Fig. 4. It can be seen that when the TE-polarized component is higher than TM-polarized component, the LEDs' LEE using the microstructure optimized for TE-polarized light is larger than that for TM-polarized light. Therefore, when the proportion of TE-polarized light is less than 21.5%, although the LEE emitted by TE-polarized is higher, the microstructure of the maximum LEE is the best result of TM-polarized emission due to the relatively small proportion of TE-polarized light. Therefore, in the design process of surface microstructure for the UVC-LEDs with a shorter emission wavelength, it is necessary to consider the TM-polarized component in the emission light. That is, the surface microstructure can be optimized to maximize light extraction when the TE-polarized component is determined, which can be influenced by the factors including Al component in the well layer, the quantum well structure, and strain level for the AlGaN-based UVC-LEDs.

For comparison, the normalized far-field light distribution of the AlGaN-based UVC-LEDs with and without optimized surface microstructure is further analyzed and given in Fig. 5 for different TE-polarized component in the emission light. It can be seen that compared the UVC-LEDs with planar structure, the light output intensity has significantly improvement in all directions when the optimized surface microstructure is used. Furthermore, after using the optimized surface structure the divergence angle of the light distribution can be greatly expanded in which the emission light intensity is half of the maximum value. It is also demonstrated that the light extraction angle range greatly depends on the TE-polarized component of emission light from the UVC-LEDs with planar structure, which is from 30 to 60° to 0–50° for the full TM-polarized and full TE-polarized emission light as shown in Fig. 5(a). Moreover, for the UVC-LEDs with the optimized surface microstructure, the divergence angle is stable at about 70° with the increase of the TE-polarized component as shown in Fig. 5(b). As a result, by using the optimized surface microstructure, the extraction angle range for TE-polarized emission light is expanded from 0 to 50° to 0–70°, which is expanded from 30 to 60° to 0–70° for the TM-polarized emission light. The reason is that the light propagation path can be adjusted through the designed microstructure with

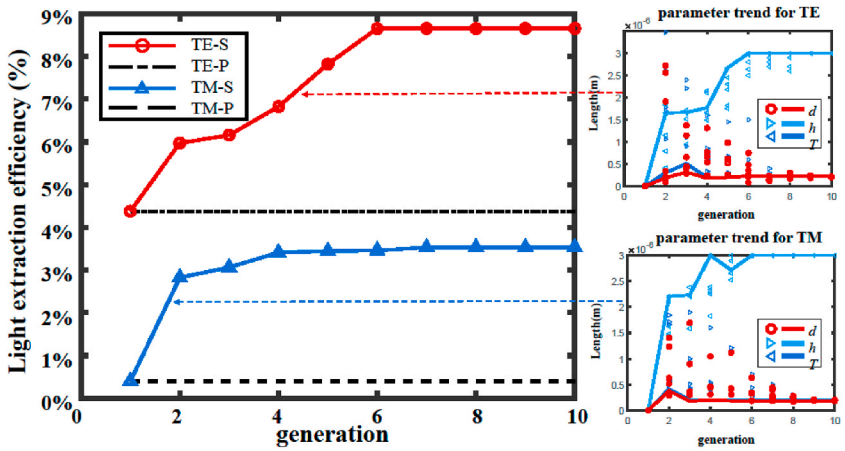

Fig. 3. Optimization process of the surface microstructure based on parabola cone array to improve light exaction and adjustment process of the structure parameter value with generation, TE/TM-S: optimized surface structure for TE/TM-polarized emission, TE/TM-P: planar structure for TE/TM-polarized emission.

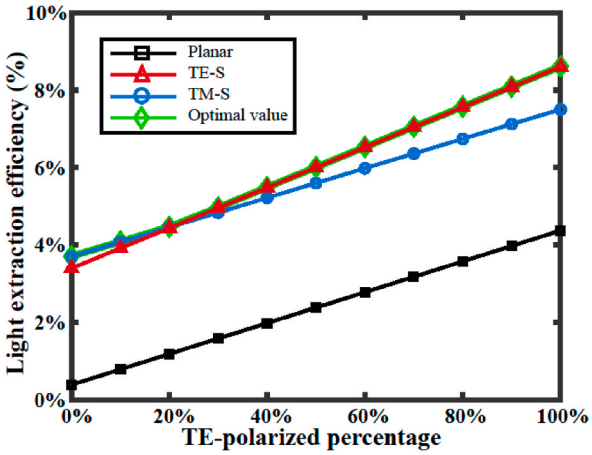

Fig. 4. The LEE value varies with the TE-polarized component for the AlGaN-based UVC-LEDs with planar surface structure and different optimized surface microstructures, TE/TM-S: optimized surface structure for TE/TM-polarized emission.

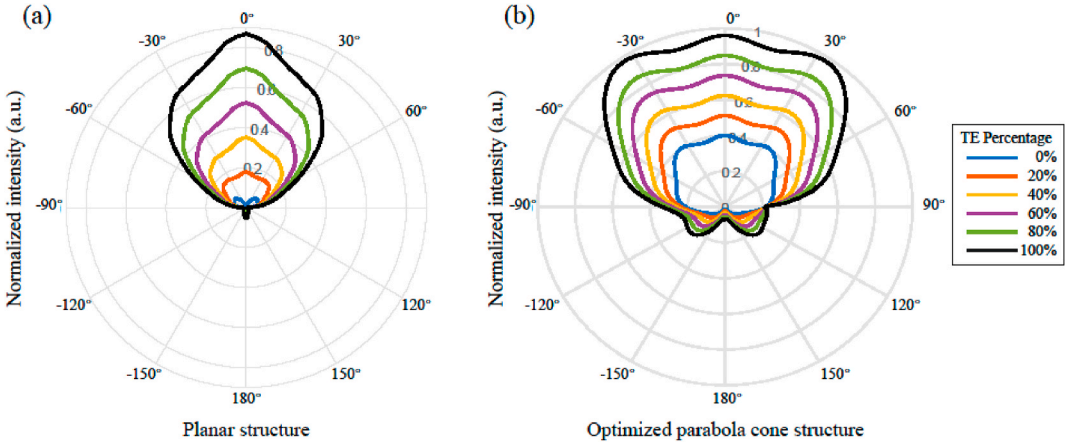

Fig. 5. Light field distribution varying with TE-polarized proportion for AlGaN-based UVC-LEDs (a) with optimized surface microstructure based on parabola cone array (b) with planar structure.

high aspect ratio and the escape cone can be enlarged. This is beneficial to the enhancement of light extraction, leading to the improvement of the LEE and EQE by using the optimized surface microstructure for the AlGaN-based UVC-LEDs.

The designed surface microstructure for light extraction improvement of AlGaN-based UVC-LEDs can be fabricated by electron beam lithography (EBL), focused ion beam (FIB) lithography, nanoimprint lithography (NIL) and other technologies. However, during the manufacturing process, there is always some microstructure deviations, including scale reduction, pattern position offset and insufficient etching depth due to the influences of various factors, such as projection lens and photomask [53,54]. In order to investigate the effect of the deviations on light extraction, the LEE was further analyzed for the UVC-LEDs with different microstructures deviation and given in Fig. 6, which is characterized by scanning of single structural parameters with cycle width *d*, height *h* and duty cycle *dr*. It can be seen from Fig. 6 that UVC-LEDs' LEE shows a slow downward trend when the parameter value of surface microstructure is close to the optimal value point. For example, when the structure width parameter smaller 10% than the optimal value, the UVC-LEDs' LEE for TE-polarized emission only decreases by 4.4%. And, there is less LEE decrease originated from other structural deviation. Therefore, the minor deviation of single structural parameter derived from fabrication process has little influence on the light extraction for the AlGaN-based UVC-LEDs with optimized surface microstructure.

Moreover, the above-mentioned deviations about scale reduction, insufficient etching depth and pattern position offset may also occur at the same time in the optimized surface microstructure for AlGaN-based UVC-LEDs. The disorder is quantified by calculating the standard deviation of the parameter values between the four nearest neighbors of each microstructure in the supercell, and then normalizing them by the parameter values of the perfectly ordered array [55,56]. As shown in Fig. 7(a), the radius decrease of microstructure bottom is expressed as deviation A related to scale reduction, deviation B correlated with insufficient etching depth is the reduction of structure height, the movement of microstructure position represented as deviation C, and deviation D randomly includes the two of above three types of deviations. For the deviation D including different combination of microstructure deviation,

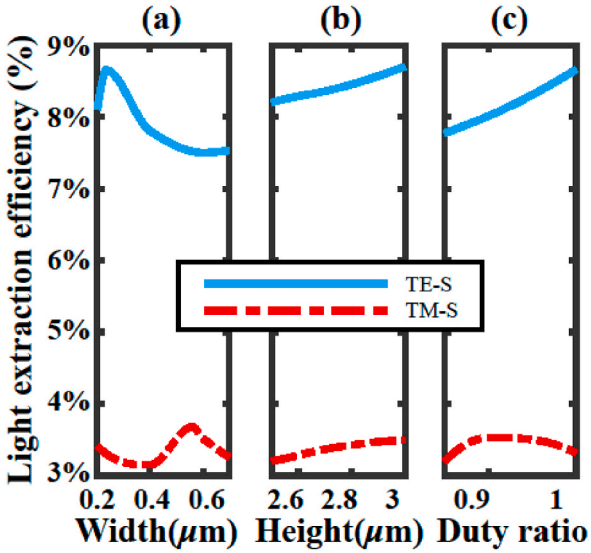

Fig. 6. LEE of AlGaN-based UVC-LEDs with surface microstructure based on parabola cone array varying with the parameter value of (a) cycle width, (b) height and (c) duty cycle, TE/TM-S: LEE of UVC-LEDs with optimized surface microstructure for TE/TM-polarized emission.

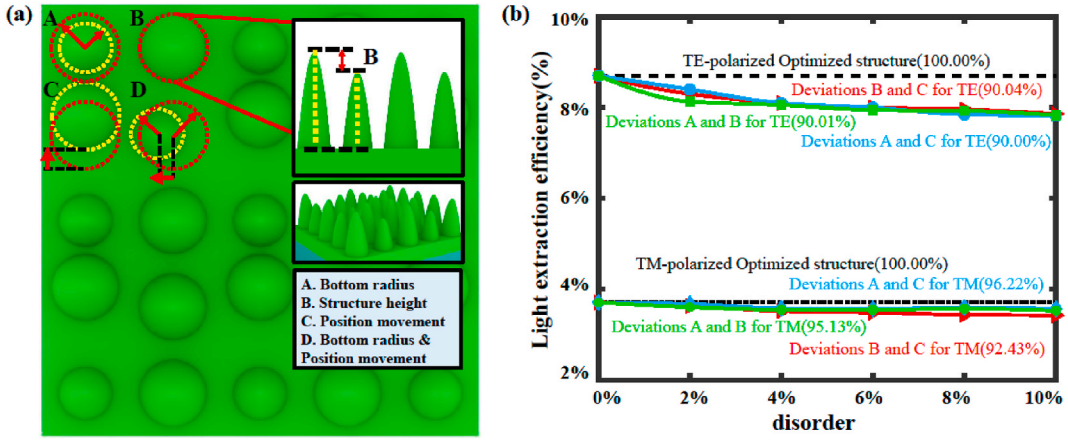

Fig. 7. (a) Deviation diagram: A bottom radius decrease, B structure height reduction, C position movement, D combination of two kinds of above deviations and (b) LEE varying with the degree of microstructure disorder.

UVC-LEDs' LEE varying with the degree of microstructure disorder is calculated and shown in Fig. 7(b). It can be seen that when the degree of disorder is less than 10%, LEE usually decreases by less than 10%, whether the surface microstructure is optimized for TE-polarized emission or for TM-polarized emission. Furthermore, the LEE decrease due to the disorder for the UVC-LEDs with TM-polarized emission is lower than that with TE-polarized emission. Therefore, for the UVC-LEDs using a designed surface microstructure with high aspect ratio, the small amplitude disorder has little effect on light extraction. As a result, the LEE improvement of AlGaN-based UVC-LEDs has a high tolerance for the manufacturing process of the optimized surface microstructure.

In addition to the changes of structural parameters caused by factors such as photolithography projection, it is difficult to control the photolithography morphology for the optimized surface microstructure with high aspect ratio. In order to characterize the influence of structural morphology on the light extraction, the LEE of AlGaN-based UVC-LEDs having optimized truncated-pyramid structure and truncated-cone structure is also analyzed, which structure diagram is shown in Fig. 8(a) comparing with that having parabola cone structure under the same structural parameter constraints[66]. Using the different surface microstructures, the corresponding UVC-LEDs' LEE results for TE-polarized and TM-polarized emission are shown in Fig. 8(b). It is revealed that the LEE of UVC-LEDs with TE-polarized emission is increased to 8.6% and 8.4% for truncated-pyramid and truncated-cone microstructure, respectively, which both has a similar increase with that for parabola cone microstructure. And, the enhancement of UVC-LEDs' LEE is close to each other for TM-polarized emission when the three different optimized surface microstructures are applied. That is, although the surface structure morphology are very different, the light extraction of UVC-LEDs can be significantly improved by using the optimized surface microstructure with high aspect ratio. Therefore, there is little influence from surface microstructure morphology on the light

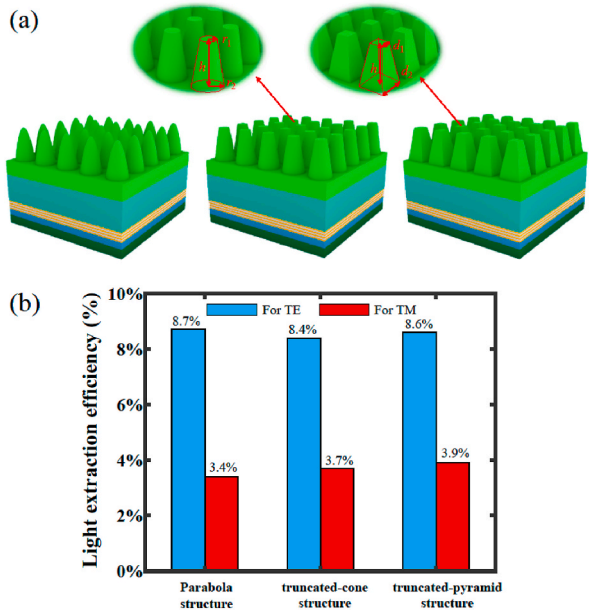

Fig. 8. (a) Schematic diagram of three kinds of surface microstructures (b) LEE results of AlGaN-based UVC-LEDs using three different surface microstructures for TE-polarized and TM-polarized emission.

extraction improvement for the AlGaN-based UVC-LEDs.

4. Conclusion

In summary, the influence of optimized surface microstructure on light extraction improvement of AlGaN-based UVC-LEDs considering optical polarization property is investigated in this work. The results showed that after using the optimized surface microstructure with high aspect ratio, the UVC-LEDs' LEE of TE-polarized and TM-polarized light can be increased by about one time and 8 times, respectively. In addition, the influence of TM polarization emission on the surface microstructure design of AlGaN based UVC LEDs was discussed. On this basis, the preparation process tolerance of the surface microstructure is discussed by calculating the UVC-LED's LEE when the structural deviation occurs or morphology changes. It is demonstrated that when the structural deviation is less than 10%, the UVC-LEDs' LEE usually decreases by less than 10% for both TE-polarized and TM-polarized emission. Furthermore, the LEE enhancement is close to each other for the UVC-LEDs with different optimized surface microstructures. That is, there is little influence from structural deviation or morphology on the light extraction improvement, which is significant to realizing high efficient short wavelength AlGaN-based UVC-LEDs by designing surface microstructures.

Funding

This work was supported by Guangdong Basic and Applied Basic Research Foundation (No. 2021B1515120086) and the National Natural Science Foundation of China (Grant No. 62234003).

Author statement

The author declares as follows:**Yifan Zhu:** Conceptualization, Methodology, Software, Validation, Formal analysis, Investigation, Resources, Data Curation, Writing - Original Draft, **Huimin Lu:** Investigation, Data Curation, Writing - Original Draft, Writing - Review & Editing, Supervision, Project administration, Funding acquisition, **Jianping Wang:** Supervision, Project administration, Funding acquisition, **Tongjun Yu:** Methodology, Resources, Supervision, **Zizheng Li:** Conceptualization, Methodology, Software, Formal analysis, Investigation, **Yucheng Tian:** Conceptualization, Methodology, Software, Validation, Formal analysis, Investigation.

Declaration of competing interest

The authors declare that they have no known competing financial interests or personal relationships that could have appeared to influence the work reported in this paper.

Data availability

Data will be made available on request.

References

[1] T.M. Robson, P.J. Aphalo, A.K. Banaś, P.W. Barnes, C.C. Brelsford, G.I. Jenkins, T.K. Kotilainen, J. Łabuz, J. Martínez-Abaigar, L.O. Morales, et al., A perspective on ecologically relevant plant-uv research and its practical application, Photochem. Photobiol. Sci. 18 (2019) 970–988.
[2] X. Luo, B. Zhang, Y. Lu, Y. Mei, L. Shen, Advances in application of ultraviolet irradiation for biofilm control in water and wastewater infrastructure, J. Hazard Mater. 421 (2022), 126682.
[3] M. Otto, M. Bender, B. Hadam, B. Spangenberg, H. Kurz, Characterization and application of a uv-based imprint technique, Microelectron. engineering 57 (2001) 361–366.
[4] C. Ribeiro, B. Alvarenga, et al., Prospects of uv radiation for application in postharvest technology, Emir. J. Food Agric. (2012) 586–597.
[5] P. Tian, X. Shan, S. Zhu, E. Xie, J.J. McKendry, E. Gu, M.D. Dawson, Algan ultraviolet micro-leds, IEEE J. Quant. Electron. 58 (2022) 1–14.
[6] R.K. Mondal, S. Adhikari, V. Chatterjee, S. Pal, Recent advances and challenges in algan-based ultra-violet light emitting diode technologies, Mater. Res. Bull. 140 (2021), 111258.
[7] T. Fukui, T. Niikura, T. Oda, Y. Kumabe, H. Ohashi, M. Sasaki, T. Igarashi, M. Kunisada, N. Yamano, K. Oe, et al., Exploratory clinical trial on the safety and bactericidal effect of 222-nm ultraviolet c irradiation in healthy humans, PLoS One 15 (2020), e0235948.
[8] K. Narita, K. Asano, Y. Morimoto, T. Igarashi, A. Nakane, Chronic irradiation with 222-nm uvc light induces neither dna damage nor epidermal lesions in mouse skin, even at high doses, PLoS One 13 (2018), e0201259.
[9] N. Yamano, M. Kunisada, S. Kaidzu, K. Sugihara, A. Nishiaki-Sawada, H. Ohashi, A. Yoshioka, T. Igarashi, A. Ohira, M. Tanito, et al., Long-term effects of 222-nm ultraviolet radiation c sterilizing lamps on mice susceptible to ultraviolet radiation, Photochem. Photobiol. 96 (2020) 853–862.
[10] W. Taylor, E. Camilleri, D.L. Craft, G. Korza, M.R. Granados, J. Peterson, R. Szczpaniak, S.K. Weller, R. Moeller, T. Douki, et al., Dna damage kills bacterial spores and cells exposed to 222-nanometer uv radiation, Appl. Environ. Microbiol. 86 (2020), e03039–19.
[11] J. Cartwright, The potential of far-uv for the next pandemic, Phys. World 33 (2020) 28.
[12] L. Guo, Y. Guo, J. Wang, T. Wei, Ultraviolet communication technique and its application, J. Semiconduct. 42 (2021), 081801.
[13] M. Guttmann, F. Mehnke, B. Belde, F. Wolf, C. Reich, L. Sulmoni, T. Wernicke, M. Kneissl, Optical light polarization and light extraction efficiency of algan-based leds emitting between 264 and 220 nm, Jpn. J. Appl. Phys. 58 (2019) SCCB20.
[14] N. Lobo-Ploch, F. Mehnke, L. Sulmoni, H.K. Cho, M. Guttmann, J. Glaab, K. Hilbrich, T. Wernicke, S. Einfeldt, M. Kneissl, Milliwatt power 233 nm algan-based deep uv-leds on sapphire substrates, Appl. Phys. Lett. 117 (2020), 111102.
[15] M. Jo, Y. Itokazu, H. Hirayama, Milliwatt-power far-uvc algan leds on sapphire substrates, Appl. Phys. Lett. 120 (2022), 211105.
[16] S. Islam, V. Protasenko, K. Lee, S. Rouvimov, J. Verma, H. Xing, D. Jena, Deep-uv emission at 219 nm from ultrathin mbe gan/aln quantum heterostructures, Appl. Phys. Lett. 111 (2017), 091104.
[17] A. Yoshikawa, R. Hasegawa, T. Morishita, K. Nagase, S. Yamada, J. Grandusky, J. Mann, A. Miller, L.J. Schowalter, Improve efficiency and long lifetime uvc leds with wavelengths between 230 and 237 nm, APEX 13 (2020), 022001.
[18] N. Susilo, E. Ziffer, S. Hagedorn, L. Cancellara, C. Netzel, N.L. Ploch, S. Wu, J. Rass, S. Walde, L. Sulmoni, et al., Improved performance of uvc-leds by combination of high-temperature annealing and epitaxially laterally overgrown aln/sapphire, Photon. Res. 8 (2020) 589–594.
[19] Z.-H. Zhang, J. Kou, S.-W.H. Chen, H. Shao, J. Che, C. Chu, K. Tian, Y. Zhang, W. Bi, H.-C. Kuo, Increasing the hole energy by grading the alloy composition of the p-type electron blocking layer for very high-performance deep ultraviolet light-emitting diodes, Photon. Res. 7 (2019) B1–B6.
[20] R.T. Velpula, B. Jain, H.Q.T. Bui, F.M. Shakiba, J. Jude, M. Tumuna, H.-D. Nguyen, T.R. Lenka, H.P.T. Nguyen, Improving carrier transport in algan deep-ultraviolet light-emitting diodes using a strip-in-a-barrier structure, Appl. Opt. 59 (2020) 5276–5281.
[21] K. Ban, J.-i. Yamamoto, K. Takeda, K. Ide, M. Iwaya, T. Takeuchi, S. Kamiyama, I. Akasaki, H. Amano, Internal quantum efficiency of whole-composition-range algan multiquantum wells, Appl. Phys. Exp. 4 (2011), 052101.
[22] Y. Sun, F. Xu, N. Zhang, J. Lang, J. Wang, B. Liu, L. Wang, N. Xie, X. Fang, X. Kang, et al., Realization of high efficiency algan-based multiple quantum wells grown on nano-patterned sapphire substrates, CrystEngComm 23 (2021) 1201–1206.
[23] M. Kneissl, T.-Y. Seong, J. Han, H. Amano, The emergence and prospects of deep-ultraviolet light-emitting diode technologies, Nat. Photonics 13 (2019) 233–244.
[24] J. Zheng, J. Li, Z. Zhong, W. Lin, L. Chen, K. Li, X. Wang, C. Chou, S. Li, J. Kang, Effect of electrical injection-induced stress on interband transitions in high al content algan mqws, RSC Adv. 7 (2017) 55157–55162.
[25] H. Long, S. Wang, J. Dai, F. Wu, J. Zhang, J. Chen, R. Liang, Z.C. Feng, C. Chen, Internal strain induced significant enhancement of deep ultraviolet light extraction efficiency for algan multiple quantum wells grown by mocvd, Opt Express 26 (2018) 680–686.
[26] S. Zhang, Y. Zhang, N. Tang, W. Wang, X. Chen, L. Fu, C. He, Y. Lv, Z. Feng, F. Xu, et al., Compressive strain induced enhancement of transverse-electric polarized ultraviolet light emission for algan quantum wells, Superlattice. Microst. 150 (2021), 106749.
[27] N. Gao, J. Chen, X. Feng, S. Lu, W. Lin, J. Li, H. Chen, K. Huang, J. Kang, Strain engineering of digitally alloyed aln/gan nanorods for far-uvc emission as short as 220 nm, Opt. Mater. Express 11 (2021) 1282–1291.
[28] C. Reich, M. Guttmann, M. Feneberg, T. Wernicke, F. Mehnke, C. Kuhn, J. Rass, M. Lapeyrade, S. Einfeldt, A. Knauer, et al., Strongly transverse-electric-polarized emission from deep ultraviolet algan quantum well light emitting diodes, Appl. Phys. Lett. 107 (2015), 142101.
[29] C. Liu, Y.K. Ooi, S. Islam, J. Verma, H. Xing, D. Jena, J. Zhang, Physics and polarization characteristics of 298 nm aln-delta-gan quantum well ultraviolet light-emitting diodes, Appl. Phys. Lett. 110 (2017), 071103.
[30] C. Liu, Y.K. Ooi, S. Islam, H. Xing, D. Jena, J. Zhang, 234 nm and 246 nm aln-delta-gan quantum well deep ultraviolet light-emitting diodes, Appl. Phys. Lett. 112 (2018), 011101.
[31] H. Wang, L. Fu, H. Lu, X. Kang, J. Wu, F. Xu, T. Yu, Anisotropic dependence of light extraction behavior on propagation path in algan-based deep-ultraviolet light-emitting diodes, Opt Express 27 (2019) A436–A444.
[32] M. Guttmann, A. Susilo, L. Sulmoni, N. Susilo, E. Ziffer, T. Wernicke, M. Kneissl, Light extraction efficiency and internal quantum efficiency of fully uvc-transparent algan based leds, J. Phys. D Appl. Phys. 54 (2021), 335101.
[33] H. Zhang, W. Zhang, S. Zhang, M. Shan, Z. Zheng, A. Wang, L. Xu, F. Wu, J. Dai, C. Chen, Improved reliability of algan-based deep ultraviolet led with modified reflective n-type electrode, IEEE Electron. Device Lett. 42 (2021) 978–981.
[34] P. Manley, S. Walde, S. Hagedorn, M. Hammerschmidt, S. Burger, C. Becker, Nanopatterned sapphire substrates in deep-uv leds: is there an optical benefit? Opt Express 28 (2020) 3619–3635.
[35] R. Floyd, M. Gaevski, M.D. Alam, S. Islam, K. Hussain, A. Mamun, S. Mollah, G. Simin, M. Chandrashekhar, A. Khan, An opto-thermal study of high brightness 280 nm emission algan micropixel light-emitting diode arrays, APEX 14 (2020), 014002.
[36] K.R. Son, B.R. Lee, M.H. Jang, H.C. Park, Y.H. Cho, T.G. Kim, Enhanced light emission from algan/gan multiple quantum wells using the localized surface plasmon effect by aluminum nanoring patterns, Photon. Res. 6 (2018) 30–36.
[37] T. Kinoshita, K. Hironaka1, T. Obata1, T. Nagashima, R. Dalmau, R. Schlesser, B. Moody, J. Xie, S. Inoue, Y. Kumagai, Deep-ultraviolet light-emitting diodes fabricated on AlN substrates prepared by hydride vapor phase epitaxy, APEX 5 (12) (2012), 122101.
[38] S. Inoue, N. Tamari, M. Taniguchi, 150 mW deep-ultraviolet light-emitting diodes with large-area AlN nanophotonic light-extraction structure emitting at 265 nm, Appl. Phys. Lett. 110 (14) (2017), 141106.

[39] S. Islam, K. Lee, J. Verma, V. Protasenko, S. Rouvimov, S. Bharadwaj, H. Xing, D. Jena, MBE-grown 232–270nm deep-uv leds using monolayer thin binary GaN/AlN quantum heterostructures, Appl. Phys. Lett. 110 (4) (2017), 041108.
[40] Y. Zhang, J. Zhang, Y. Zheng, C. Sun, K. Tian, C. Chu, Z.-H. Zhang, J.G. Liu, W. Bi, The effect of sapphire substrates on omni-directional reflector design for flip-chip near-ultraviolet light-emitting diodes, IEEE Photon. J. 11 (2019) 1–9.
[41] Y. Zhang, Y. Zheng, R. Meng, C. Sun, K. Tian, C. Geng, Z.-H. Zhang, G. Liu, W. Bi, Enhancing both tm-and te-polarized light extraction efficiency of algan-based deep ultraviolet light-emitting diode via air cavity extractor with vertical sidewall, IEEE Photon. J. 10 (2018) 1–9.
[42] I. Vurgaftman, J.n. Meyer, Band parameters for nitrogen-containing semiconductors, J. Appl. Phys. 94 (2003) 3675–3696.
[43] H.-Y. Ryu, I.-G. Choi, H.-S. Choi, J.-I. Shim, Investigation of light extraction efficiency in algan deep-ultraviolet light-emitting diodes, APEX 6 (2013), 062101.
[44] H.-Y. Ryu, Large enhancement of light extraction efficiency in algan-based nanorod ultraviolet light-emitting diode structures, Nanoscale Res. Lett. 9 (2014) 1–7.
[45] T. Wei, X. Ji, K. Wu, H. Zheng, C. Du, Y. Chen, Q. Yan, L. Zhao, Z. Zhou, J. Wang, et al., Efficiency improvement and droop behavior in nanospherical-lens lithographically patterned bottom and top photonic crystal ingan/gan light-emitting diodes, Opt. Lett. 39 (2014) 379–382.
[46] Y. Zhang, T. Wei, Z. Xiong, L. Shang, Y. Tian, Y. Zhao, P. Zhou, J. Wang, J. Li, Enhanced optical power of gan-based light-emitting diode with compound photonic crystals by multiple-exposure nanosphere-lens lithography, Appl. Phys. Lett. 105 (2014), 013108.
[47] T. Wei, K. Wu, D. Lan, Q. Yan, Y. Chen, C. Du, J. Wang, Y. Zeng, J. Li, Selectively grown photonic crystal structures for high efficiency ingan emitting diodes using nanospherical-lens lithography, Appl. Phys. Lett. 101 (2012), 211111.
[48] M. Djavid, Z. Mi, Enhancing the light extraction efficiency of algan deep ultraviolet light emitting diodes by using nanowire structures, Appl. Phys. Lett. 108 (2016), 051102.
[49] R.P. Singh, M. Dixit, S. Silakari, Image contrast enhancement using ga and pso: a survey, in: International Conference on Computational Intelligence and Communication Networks, IEEE, 2014, pp. 186–189, 2014.
[50] J. Tang, G. Liu, Q. Pan, A review on representative swarm intelligence algorithms for solving optimization problems: applications and trends, IEEE/CAA J. Autom. Sinica 8 (2021) 1627–1643.
[51] A. Slowik, H. Kwasnicka, Nature inspired methods and their industry applications—swarm intelligence algorithms, IEEE Trans. Ind. Inf. 14 (2017) 1004–1015.
[52] Y. Zhu, H. Lu, J. Wang, T. Yu, Z. Li, Y. Tian, Enhanced light extraction by optimizing surface microstructure for algan-based deep ultraviolet light emitting diodes with 265 and 280 nm emission, J. Appl. Phys. 132 (2022), 225704.
[53] C. Wagner, N. Harned, Lithography gets extreme, Nat. Photonics 4 (2010) 24–26.
[54] M. Blaicher, M.R. Billah, J. Kemal, T. Hoose, P. Marin-Palomo, A. Hofmann, Y. Kutuvantavida, C. Kieninger, P.-I. Dietrich, M. Lauermann, et al., Hybrid multi-chip assembly of optical communication engines by in situ 3d nano-lithography, Light Sci. Appl. 9 (2020) 71.
[55] A. Ushkov, O. Dellea, I. Verrier, T. Kampfe, A. Shcherbakov, J.-Y. Michalon, Y. Jourlin, Compensation of disorder for extraordinary optical transmission effect in nanopore arrays fabricated by nanosphere photolithography, Opt Express 28 (2020) 38049–38060.
[56] P. Moitra, B.A. Slovick, Z. Gang Yu, S. Krishnamurthy, J. Valentine, Experimental demonstration of a broadband all-dielectric metamaterial perfect reflector, Appl. Phys. Lett. 104 (2014), 171102.